Neuromorphic VLSI realization of the Hippocampal Formation

Anu Aggarwal
University of Maryland,
College Park, MD, USA
Email: aaagganu@gmail.com

Abstract—The medial entorhinal cortex grid cells, aided by the subicular head direction cells, are thought to provide a matrix which is utilized by the hippocampal place cells for calculation of position of an animal during spatial navigation. The place cells are thought to function as an internal GPS for the brain and provide a spatiotemporal stamp on episodic memories. Several computational neuroscience models have been proposed to explain the place specific firing patterns of the cells of the hippocampal formation – including the GRIDSmap model for grid cells and Bayesian integration for place cells. In this work, we present design and measurement results from a first ever system of silicon circuits which successfully realize the function of the hippocampal formation of brain based on these models.

Keywords— Silicon hippocampal formation, Grid cells, Stripe cells, GRIDSmap model, Place cells, Bayesian integration synapse

1 INTRODUCTION

Spatial navigation is quintessential to the survival of a species. For successful spatial navigation, information about the direction and distance of the target w.r.t. current position of the animal is needed. In conventional navigation, e.g., that with a global positioning system (GPS), a fixed map of the environment is used to achieve this. In contrast, the autonomous robotic spatial navigation requires exploration of a new or a changing environment, which needs dynamic spatial maps of the environment which update constantly based on new information from the environment. The hippocampal formation is a part of the nervous system which is thought to be involved in spatial navigation [1], [2] by storing spatial maps of the environment in memory and constantly updating them by integrating new spatial information. Thus, silicon implementation of the hippocampal formation could provide a mechanism for autonomous robotic spatial navigation. There have been prior attempts [3], [4] at building parts of the system in silicon but none of them have been able to achieve the functionality fully. Therefore, in this paper we propose a system in silicon which successfully realizes the function of the hippocampal formation.

2 CELLS OF THE HIPPOCAMPAL FORMATION

Anatomically, the human hippocampal formation is a C-shaped structure, located on the medial aspect of the cerebral hemispheres. It consists of the subiculum, the medial and lateral entorhinal cortices and the hippocampus proper, among other regions. In [5], [6], [7], existence of head direction cells in the subiculum, which fired when the head of the animal was pointing in a particular direction (w.r.t. orienting cues) or within 45 degrees thereof, was presented. Functionally, these cells can provide an estimate of the heading direction of the animal. In [8], grid cells in the medial entorhinal cortex were demonstrated as firing when the animal is located at the corners of equilateral triangles in space. The firing pattern of a grid cell repeats over the entire surface as the animal moves around, thus, providing a matrix which spans the environment. The neighbouring grid cells show similar spacing, field size and orientation but differ in their vertex locations. The spatial frequency of the grid firing pattern increases along the dorso-ventral axis of the medial entorhinal cortex, i.e., the cells located more ventrally have more widely distributed fields. This scaling varies from 30-45 cm in the most dorsal to about 1 to several metres in the most ventral region. Place cells are the pyramidal cells in the hippocampus which fire whenever the animal is at a particular location in space [9]-[14]. As such ensembles of place cells provide a spatial map of the environment. They are also involved in encoding a ‘space and time stamp’ on newly created episodic memories. Thus, the hippocampal formation of the brain functions as a self-learning internal GPS with ability to dynamically update memory. Several mathematical models have been proposed to explain these place specific firing patterns of the hippocampal cells, some of which we used in our silicon implementation of the hippocampal formation. These are presented in the next section.

3 MODELS OF THE HIPPOCAMPAL FORMATION

To design our system in silicon, we used the GRIDSmap model for grid cells and Bayesian integration for place cells which are described in this section.

3.1 *Grid cell Models*

The GRIDSmap (Grid Regularity from Integrated Distance through Self-organizing map) model [21] was used to implement our silicon realization of the grid cell system because it describes the grid cell spatial firing pattern based on trigonometric principles which maps the entire space on to 3 rings of stripe cells. According to this model, the rings of stripe cells are present in layer III of the entorhinal cortex and provide input to the grid cells located in layer II of the entorhinal cortex. Each grid cell receives inputs from a stripe cell on three different rings whose preferred firing directions are oriented at 120 degrees to each other. These stripe cells perform velocity integration along their preferred direction. As the animal moves around in the environment, the distance covered by it is projected onto these stripe cells using the trigonometric principles (Fig. 1). For instance, if the animal is at point A in space, which corresponds to (1, 1) in the x-y plane, then the distance, *r* from the origin is 1.414 m. And that along each of the three axis is *r**cos θ, where θ is the angle subtended by the axis to the vector pointing in the direction of A. This distance wraps around as the number of stripe cells is limited. The distance after which this wrapping around occurs, determines the spatial firing frequency of the grid cells because the grid cell fires only when inputs to it from all the three rings are coincident (Fig. 1 (d)). Since the rings are aligned at 120 degrees to each other, the grid spatial firing pattern is hexagonal with additional firing at the center of the hexagon (or firing at the corners of an equilateral triangle). To demonstrate spatial firing patterns with different frequencies in our silicon system, one way could be to connect different number of neurons in the rings to the grid cell. For instance, if the motion integration along the ring wraps around every 1m, then connecting the same neuron number on each ring to a grid cell will produce a grid cell with spatial firing frequency of 1m. To implement this model in silicon, we need circuits representing three rings of stripe cells, grid cell neurons and synapses and interconnections between the two. As part of this work, we designed and tested such circuits which are presented in later sections.

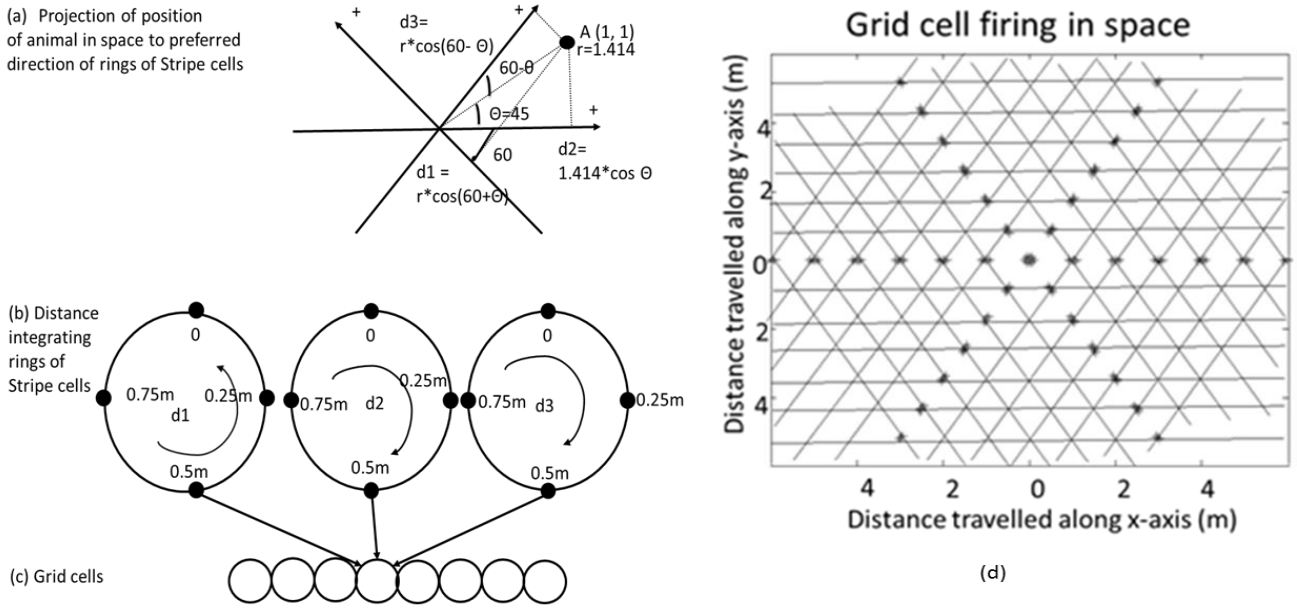

Fig. 1(a) Position of the animal is projected onto the Stripe cells ring's orientation according to the trigonometric principles. (b) Integration of distance travelled in space on to the three rings of stripe cells, one of the stripe cells from each ring is connected to a (c) grid cell (d) Firing of a grid cell at coincidence of inputs from the 3 stripe cells (with preferred orientations at 120 degrees to each other). This pattern repeats as the distance travelled along each direction wraps around the ring.

In addition to the GRIDSmap model, there are two other widely accepted models explaining the grid cell firing patterns – the attractor dynamic [2], [15], and the oscillatory interference [18], [19]. The attractor dynamic model was not used for silicon implementation because a variation of this was attempted for implementation in silicon [4] in which authors reported their inability to move the grid pattern around during motion integration. Moreover, the silicon implementation of this model requires a huge overhead of software interfaces. Therefore, we did not use this model for our system implementation. The oscillatory interference (OI) model or its extension [20] were not used for our system implementation as these use velocity and not distance integration. Moreover, they explain motion only along the three axis of preference of the three head direction cells and not for the spaces in between these axis.

3.2 *Place cell Models*

Several models have been proposed to explain the place specific firing patterns of the hippocampal pyramidal cells both in the pre grid and the post grid cell era. In the pre grid cell era, place cell firing was thought to depend upon sensory inputs alone. These manifested as the relative distance of the animal from a landmark, or as fixed distance from the boundary vector cells (BVCs) which fire when the animal is either along the boundaries of the enclosure or along a partition in the enclosure [22], [23]. However, this model holds little appeal in explaining place cell firing in the post grid cell era because it does not take motion integration by grid cells into account while primary source of inputs to the hippocampus (seat of place cells) is the medial entorhinal cortex (seat of grid cells). After the demonstration of regular spatial firing patterns of the grid cells, models proposed (including the attractor dynamic, the oscillatory interference and the GRIDSmap) assign integration of inputs of grid cells (integrated motor inputs) of varying spatial frequencies to be the cause of place cell firing. Another category of models is based on networks of synapses with different weights connecting grid to place cells and generating place cell firing patterns based on learning rules like Hebbian learning, independent component analysis or other competitive learning mechanisms [15], [24]-[33]. In [34], it has been postulated that grid cells by performing path integration, influence the place cell firing primarily in dark while environmental cues influence the firing in light. In [35], the authors contended that the place and the grid cells cooperate to provide accurate spatial mapping of the environment. Though different in their approach, all the current models assign integration of grid cell inputs of varying spatial firing frequencies as the cause for place cell firing. In a recent study [44], it has been contended that this integration could possibly occur in a Bayes' optimal manner. This is explained in detail in the next section.

3.3 *Bayesian integration of inputs at the place cell*

Bayesian integration means that the information from different sources is combined by weighing it according to its accuracy, i.e. more precise information receives a higher weight. Mathematically, it can be represented as

$$p(x \mid O) \propto p(x) * p(O \mid x) \qquad (1)$$

Where x is the animal's location in space and O= $\{o_1, \ldots o_N\}$ represents a set of firings of the place cell. Thus, this needs multiplication of different probability distributions. The probabilities on the left and the right hand sides of equation (1) are equal if the *p(O)* is the same everywhere. Though evidence of information integration in brain based on Bayesian mechanism has been postulated for neuronal ensembles [36]-[43], it has not been shown to exist at a single cell level except for in [44]. Here, it is contended that as seen in neuronal ensembles elsewhere in the brain, Bayesian integration could also be the mechanism for integration of inputs from many sources inside single place cell neurons. They have contended that though the results do not fit the data exactly, the model is simple and fits the data reasonably well[1]. Hence, this concept of Bayesian integration is entirely different from that performed by networks of multiple neurons. They have used simulations to explain integration of external and internal cues as per the BVC model. In this work, we extend this concept to the GRIDSmap model.

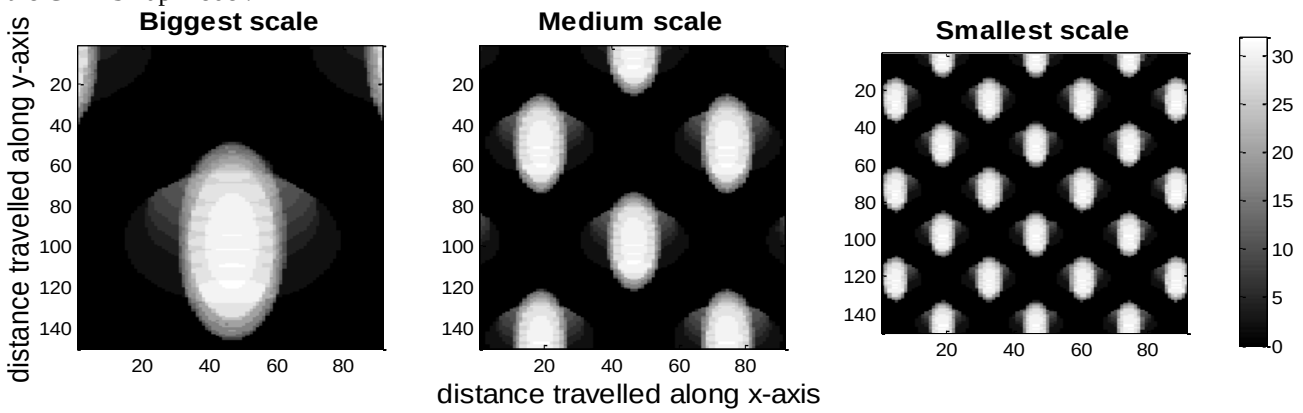

Fig. 2 Matlab simulation of the GRIDSmap model producing grid cell spatial firing patterns with different frequencies. These are similar to the spatial firing frequencies which have been observed during recordings from live lab animals.

[1] According to the Madl's model, the place cells perform Bayesian integration at the single cell level which if implemented in hardware shall be represented as coincidence detection rather than as stochastic response (seen traditionally) where groups of neurons (and not a single neuron) perform Bayesian integration.

For testing it, we did MATLAB [45] simulations of the animal motion in free space based on this model. Simulating the motion of animal in free space, we obtained the grid cell firing pattern in space as predicted by the GRIDSmap model. As seen in Fig. 2, the firing patterns had a Gaussian shape of a probability distribution, i.e., the firing rates were higher in the center and lower at the periphery. Thereafter, we performed Bayesian integration on these probability distributions (by multiplying them in MATLAB). Results (
Fig. 3(b)) show that the Bayesian integration of grid cell inputs can produce a localized field - as observed empirically. This is in contrast to place cell firing due to summation and thresholding of inputs from grid cells (
Fig. 3(a)) which produces multiple foci of firing for a place cell within an environment which is not what is observed empirically. Hence, we also agree with the proposal of [44] that Bayesian integration of inputs to place cells is more plausible than summation and thresholding as proposed in the GRIDSmap and other models and would like to extend it to the GRIDSmap model. Thus, to implement the function of place cells in silicon based on the GRIDSmap model and Bayesian integration of grid cell inputs, we designed a place chip with Bayesian integration synapse and conductance neuron circuits. This is described in subsequent sections.

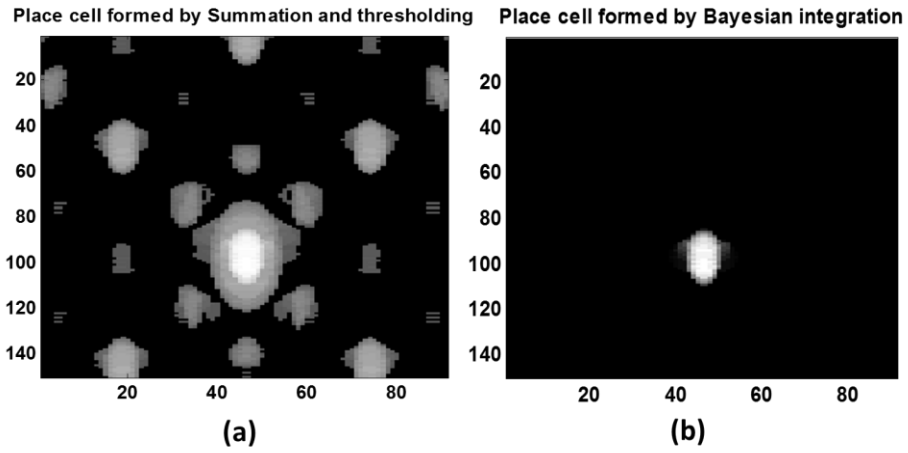

Fig. 3 MATLAB simulation results of place cell firing produced (a) by summation and thresholding of inputs from grid cells with different spatial firing frequencies, as shown in figure above, and (b) by Bayesian integration of the same grid cell inputs. The latter corresponds more closely to empirical observations.

4 System description

The entire silicon hippocampal formation was built using three silicon chips – the stripe cell ring chip, the grid chip and the place chip, connected through software interfaces designed in Verilog and implemented on a Nexys2 Spartan 3E FPGA board (

Fig. 4). Each stripe cell chip had 12 ring circuits, each grid chip had 24 conductance neuron and second order synapse circuits and each place chip had 8 Bayesian integration synapses and conductance neurons integrated on them.

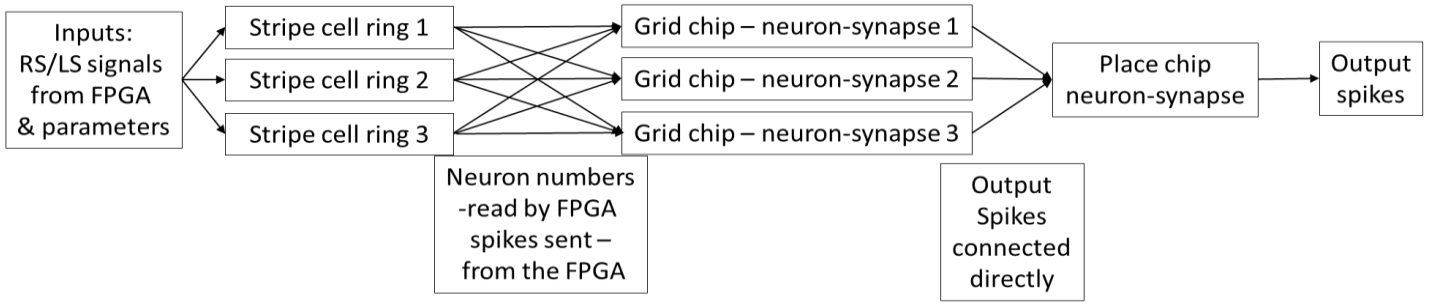

Fig. 4 Schematic of the system of chips used to achieve the function of the electronic hippocampal formation.

To build the hippocampal formation from these chips, 3 ring circuits (1 from each of the stripe cell ring chips) with 24 nodes and 24 neurons, 3 grid synapse-neuron (1 from each of the grid chips) and 1 place synapse-neuron circuits were used and connected through software interfaces built in FPGA. Animal motion in space was simulated and mapped on to the 3 ring circuits based on the GRIDSmap model described above. Position of the active node on the rings was moved around by providing right shift (*RS*) and left shift (*LS*) signals to the ring circuits. Projection of animal motion along the rings was wrapped around after every 1 m. Thus, to get a particular grid cell spatial firing frequency, we connected 1 stripe cell (say 24) on all the three rings to a grid cell and set the grid cell's firing threshold such that it fired only when it received inputs from all the rings simultaneously. To obtain half of that spatial firing frequency, we connected it to 2 of the equidistant nodes (say 12, 24) of the three rings. Similarly, to obtain a fourth of the spatial firing frequency for a grid cell, we connected 4 equidistant nodes (say 6, 12, 18 and 24) on all the rings to the grid cell. From this, we could realize the function of three grid cells with different spatial firing frequencies. We integrated the outputs of these three cells using the Bayesian integration synapse onto a conductance neuron circuit which functioned as a place cell. The software interfaces were designed to make the system flexible (for instance, testing different combinations of inputs to grid and place cells) and were deliberately introduced and not as a substitute to hardware circuits.

5 CIRCUITS

As mentioned above, the system was designed using the stripe cell ring chip, the grid chip and the place chip. To reduce the area and power consumption by the circuits, the system was implemented using only a few circuits on each chip such that in future implementations of the system, the entire system can be integrated on a single tiny chip unit[2]. Circuits on these chips (even though for different applications) have been published in [46], [49], [51].

5.1 *The stripe cell ring chip*

Each stripe cell ring chip (

Fig. 5) had 12 ring circuits integrated on it along with the 5 to 24 line decoder (to route inputs), the address event representation (AER[3]) [48], and 24 to 5 bit encoder for reading neuron/node addresses from the ring. The decoder circuit was used to route *RS/LS* (right shift/left shift) signals to this ring to move the node of activity around. Encoder circuit was also used to read the neuron number which was firing. Of the 12 rings on each chip, only 1 was used. The others could not be used because the AER circuit could not read the ring addresses sequentially as required to implement the GRIDSmap model. This did not get caught at the simulation stage as the PSPICE simulations did not have enough bandwidth. So, to use 3 ring circuits for the system, 1 circuit from a chip was used. This did not affect the functionality of the system in any manner.

[2] Tiny chip unit is a standard size of chip fabricated by MOSIS. The dimensions of the chip are 1.275mmX1.275 mm.

[3] Address event representation circuit is an asynchronous digital circuit used to process spiking inputs. It is required because in silicon implementation of neuronal ensembles, we need to read spiking outputs from several neurons which fire simultaneously without losing information from any of them. The circuit can receive several inputs and randomly (and not sequentially) select between the one that it processes. Processing involves reading the neuron number which is firing. For all its functions, the circuit has 3 sub-circuits in it – the arblogic, the arbiter and the encoder. The arblogic and the arbiter, randomly select the spiking input which is processed at a time and then send it to the encoder which converts the neuron number into a digital address.

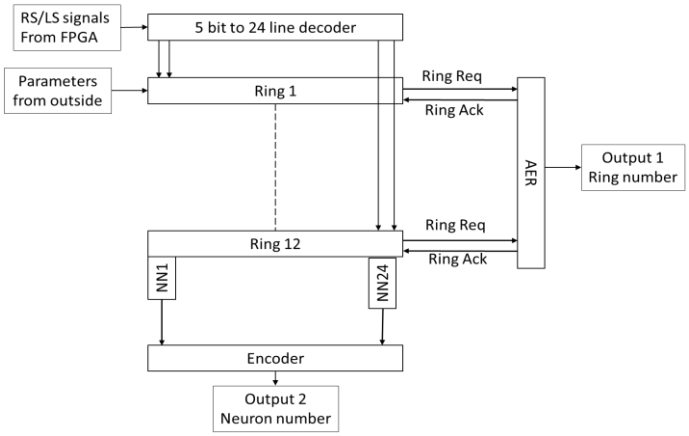

Fig. 5 Schematic showing arrangement of circuits on the stripe cell ring chip

Each ring circuit had two parts: a winner take all (WTA) [47] circuit with 24 nodes and 24 integrate and fire neurons (
Fig. 6). The WTA circuit was used to make the ring circuit compact and power efficient, the neurons were used to communicate the winning node position as neuronal firing to the encoder and AER circuits which could read its address. As per the WTA circuit, only one node wins at a time. The first node was designed differently with provision for reset which helps it to be the winning node whenever the ring is reset. The reset signal chooses between *V1* and *V2* and here, *V1* was kept at a lower value than *V2*. Once this node wins, it stays as the winner as long as the parameters *RS* and *LS* are held at 0V. During this time, the *M5-M6* current mirror copies the current from the winning node to the connected capacitor which charges up to *Vdd*. The current is controlled by *cCon* applied to the gate of *M13*. The capacitors of the non-winning nodes cannot charge up due to the leak nfet (*M9*). Since the WTA circuits are prone to mismatch, *M4-M5* current mirror was used to copy the current back to the winning node (positive feedback) and help it stay winning. When *RS* is changed to *Vdd*, the charge stored in the capacitor is transferred to *N2*, which starts winning. Thus, the winning node of the ring can be reset to 0, held at a particular value for a duration of choice and moved around as is required to implement the GRIDSmap model. In this circuit, the W/L of *M4* was kept at 1/5 so that the positive feedback is not too strong to hinder movement to the next node but is strong enough to overcome potential mismatch. Another aspect of circuit design was that when the *RS* or *LS* is pulled high, a lot of charge is transferred in a very short time (1 µs). This could cause charging of all the capacitors and uncontrolled movement of the winning node if M6 is wide enough. To avoid this, W/L of M6 was kept at 1/5 so that the capacitor charges up slowly. The capacitor value was chosen to be 75fF so that it could store enough charge to overcome capacitance at the drain of *M3*, *M4*, *M7* and the gate of *M8*, which had to be raised above 2V to make the node winning. The capacitor value could not be too high as this would have fabrication constraints (1 ring with 24 nodes and 24 neurons each had to be integrated along the length (1.275 mm) of 1 tiny chip unit).

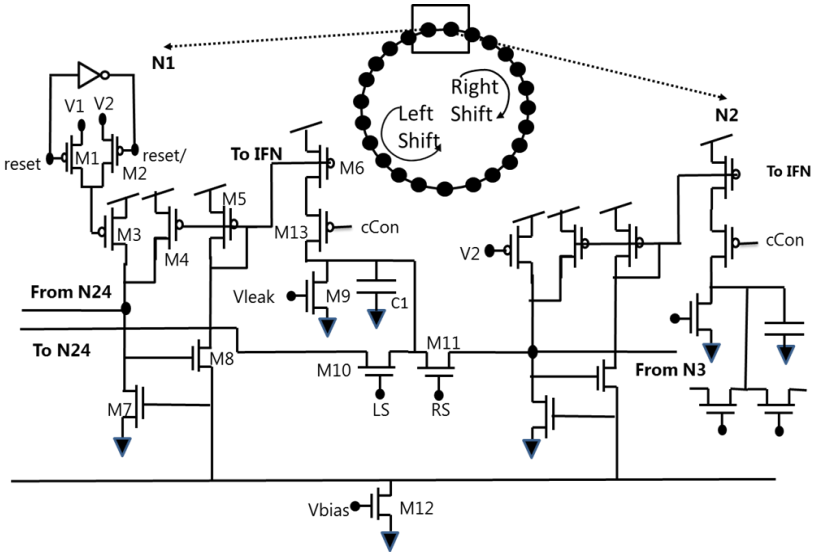

Fig. 6 Circuit schematic showing two of the 24 nodes on the stripe cell ring chip, the rest of the nodes were similar to node *N2*. Node 1, *N1* has provision for reset. W/L for M4=2.4 µm/12 µm and for the rest, it was 2.4 µm/2.4 µm. *C1*=75 fF.

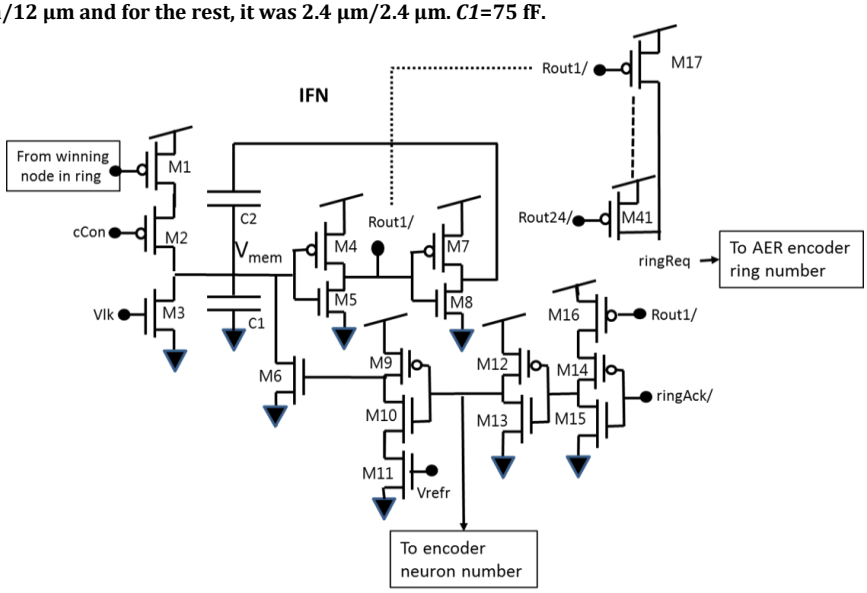

Fig. 7 Circuit schematic of the integrate and fire neuron, used to read the output current from each of the 24 nodes on the stripe cell ring circuit. C1=60fF, C2=30fF, W/L of M1=6µm/1.2µm, M11=2.4µm/2.4µm, and for the rest =1.5 µm/1.5 µm.

Each of the 24 IFN (

Fig. 7) multiplies the current, copied to it from the winning node, by 5 (W/L ratio of *M1*). To control neuronal firing, the current integrating on to *C1* was controlled by *cCon* parameter applied to the gate of *M2*. When the capacitor voltage reaches the threshold defined by the size of the nfet (*M5*) and pfet (*M4*), the neuron fires a spike, which is amplified by the gain of the two inverters. The feedback capacitor maintains the membrane potential for a while for persistent spiking. The spikes so generated from all 24 neurons on a ring were processed using a chain of pfets (*M17-M41*) whose drains were connected to the AER circuit. The AER circuit reads the ring number using a 16 to 4 encoder. Once the ring to be read is chosen, the *ackRing/* signal is sent back and the neuron number is read using the orthogonally placed 24 to 5 encoder. Once the ring and neuron numbers have been read, the neuron is reset after a refractory period determined by V_{refr}.

5.2 *The grid chip*

Based on the GRIDSmap model, the grid pattern of a particular spatial firing frequency can be demonstrated with a single grid neuron-synapse circuit where the synapse can sum the 3 inputs (from 3 stripe cell ring circuits) and present it to the grid neuron whose threshold can be set such that it fires only when it receives all the 3 inputs simultaneously. However, to demonstrate the place cell firing according to the Bayesian integration model, we need at least 2 grid cells with different spatial firing frequencies. Thus, in this project we used 3 grid synapse-neuron circuits to demonstrate the grid and the place cell firing. Moreover, to enable neuronal firing only when a grid cell gets input from all three neurons on the 3 rings simultaneously but not otherwise, we used the second order synapse circuit (
Fig. 9) which can produce output current proportional to the number of inputs. This synapse circuit was connected to the conductance neuron circuit (
Fig. 9) whose threshold can be controlled such that it fires only when the synapse circuit has produced output current proportional to 3 inputs and not just one. The grid chip had 24 of these synapse-neuron circuits on it. The inputs to the synapse circuit were routed through the 5 to 24 decoder and neuron outputs were read through the AER circuit. However, the AER processing of outputs from different synapse-neuron circuits was not sequential as required for this project. Thus, we did not use all the 24 circuits on a single chip. Instead, we used the test circuit (which was similar to other synapse-neuron circuits but had separate read in and read out which was not routed through the AER) and one other synapse-neuron circuit on one chip and a test circuit on a second chip. If we had the provision for reading the neuron outputs separately, we could have used all the 3 synapse-neuron circuits from the same chip. This can be done in future implementations of the system to save chip area.

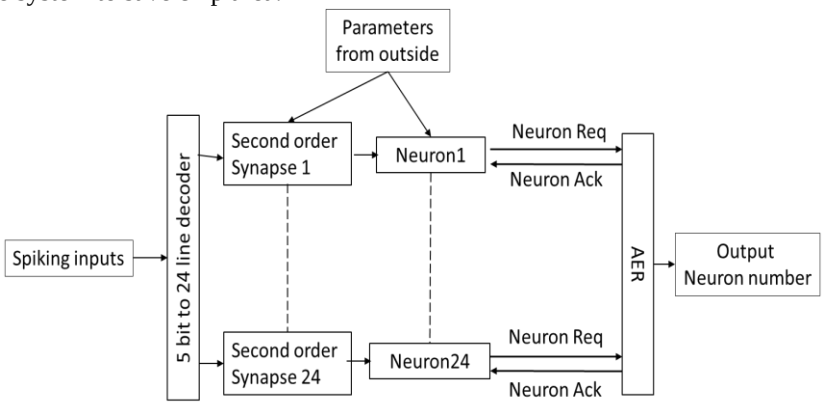

Fig. 8 Schematic showing arrangement of circuits on the grid chip

The neuron circuit ([46],
Fig. 9(a)) used for this chip has one excitatory input which pulls the membrane potential down, allowing the neuron to fire. The neuronal firing in the quiescent state is inhibited by leak current through a transistor on to the node representing the membrane potential. With constant V_{exc}, output current in steady state, I_{m_ss} will be

$$I_{m\_ss} = I_o e^{\frac{\kappa(V_{dd}-V_{we})}{V_T}} \left(\frac{I_e}{I_{lk}} \right) \qquad (2)$$

i.e., it depends directly upon the excitatory input, scaled by bias voltage (V_{we}). As the membrane potential, V_x for the neuron reaches a value which matches the V_{thr}, it fires a digital spike (R_{out}) which is amplified by the gain of the two invertors and maintained for a while by the feedback through the capacitor, C_{fb}. This R_{out} is read by the AER circuit. After firing for a while, the neuron is reset by the *ack* signal coming back from the AER circuit. The refractory period after which the neuron is ready to fire again is determined by the parameter V_{refr}, applied to the gate of *M10.*

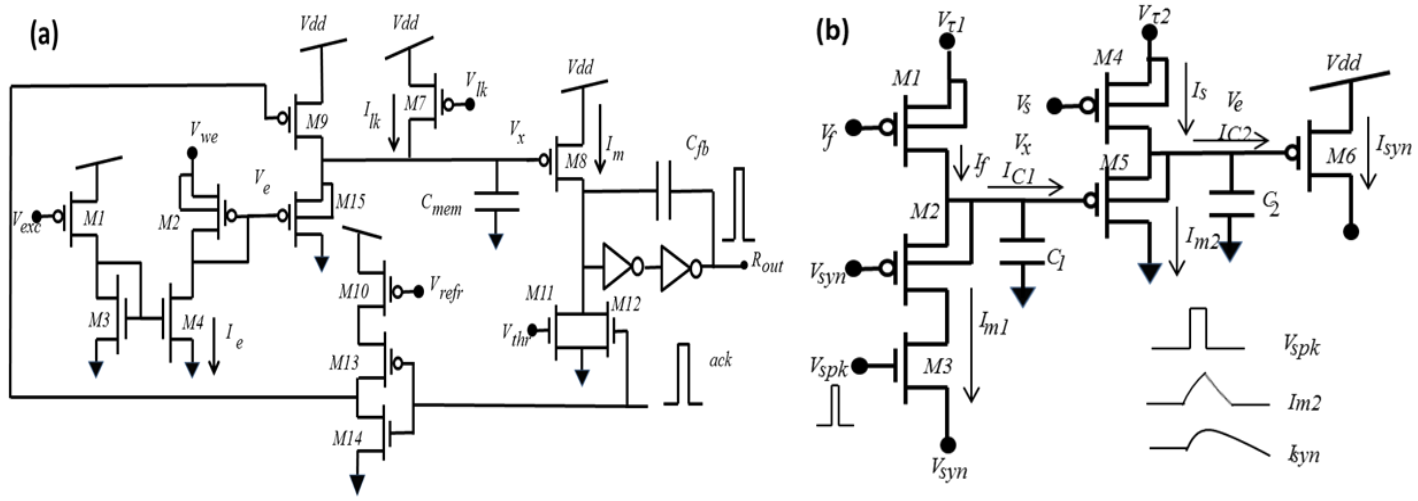

Fig. 9 Circuit of the (a) neuron (based on the Hodgkin-Huxley model of the neuron) and (b) second order synapse used in the grid chip. With no critical constraints on sizing, all transistors were 2.4µm/2.4µm and all capacitors=0.1pF.

The synapse circuit (
Fig. 9(b)) used was the second order synapse [49] which can convert a sub microsecond input pulse applied to the gate of *M3* into a second order function shaped output current, whose time constant can be varied from 0.5 to 50 ms. *M1*, *M2* and *C1* act as a first pass filter while *M4*, *M5* and *C2* work as the second pass filter. Operating in the subthreshold region, the current outputs of transistors are exponential to the gate voltages. So, using the small signal approximation of the same, the transfer function of this circuit is

$$I_{syn} = \frac{I_0^{\,3} e^{\frac{\kappa Vdd}{V_T}} e^{\frac{-\kappa V_{syn}}{V_T}}}{I_f I_s \left(1 + 2s\frac{C_1 V_T}{I_f \kappa}\right)\left(1 + s\frac{C_2 V_T}{I_s \kappa}\right)} \qquad (3)$$

In the final implementation of the system, the coincidence detection was done using the FPGA which sent a single input pulse to the grid cell synapse only if outputs from the required nodes on the three rings were coincident while time constants in the biological range were created using the second order synapse circuit which in turn were read by the neuron circuit.

5.3 *Place Chip*

Since we wanted to implement place cell firing using Bayesian integration of outputs from grid cells with different spatial firing frequencies, a Bayesian integration synapse (Fig. 11) was designed and fabricated on the place chip (
Fig. 10). This synapse circuit receives inputs from the 3 grid neurons and if inputs to it are simultaneous, the synapse produces a current output which was processed using the conductance neuron (
Fig. 9(a)) which was fabricated on the same chip. In total, this chip had 9 such synapse-neuron circuits including a test circuit. Each synapse circuit received 3 spiking inputs routed through the on chip 5 to 24 decoder circuit. The spiking outputs from the neuron circuit were read using the AER circuit.
The circuit of the Bayesian integration synapse was a current mode, sub threshold circuit, based on bump and correlator circuits (Fig. 11), [50]. The equations for the synapse circuit are

$$\mathbf{I}_{mid} = \frac{I_b}{1 + \frac{4}{S}} \qquad (4)$$

$$I_{out} = \frac{I_g(\mathrm{M1}) * I_g(M2)}{I_g(\mathrm{M1}) + I_g(M2)} \qquad (5)$$

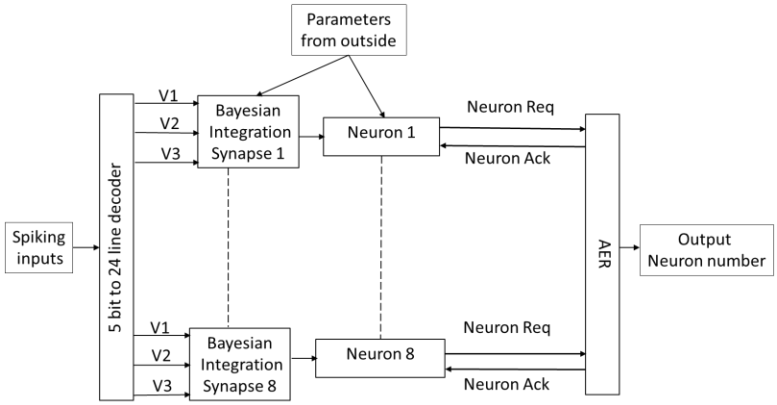

Fig. 10 Schematic showing circuit arrangements on the place chip

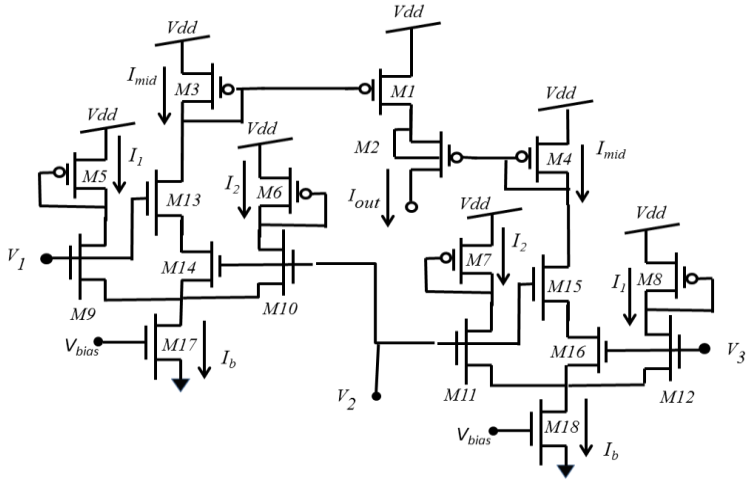

Fig. 11 Circuit schematic of the Bayesian integration synapse designed using bump and correlator circuits.

Here, the circuit performs multiplication of the spiking inputs to it from the 3 grid neurons as is required to implement Bayesian integration of inputs at the place cell. This is because in hardware, we don't have probabilities (as used for calculations in software) but actual spikes. The circuit also scales output with respect to the other inputs. Thus, with these synapse and neuron circuits, we performed Bayesian integration of inputs to implement place cell firing.

6 TESTING & RESULTS

To demonstrate the function of the hippocampal formation in silicon based on the GRIDSmap model of grid cells and the Bayesian integration, we used the chips described above. Each chip was 1.275X1.275 mm, fabricated using the commercially available ON semiconductor process from MOSIS. 3 stripe cell rings, 3 grid cells and 1 place cell were used to realize the function of the system. Custom test PCBs were designed to test these chips, and software interfaces for communication between the chips were designed using Verilog, implemented on Spartan 3E Nexys2 Digilent FPGA board. The output was recorded using Agilent MSO 6014A mixed signal oscilloscope and then processed in MATLAB [45].

To demonstrate the function of the silicon system as hippocampal formation, we provided spiking inputs (*RS* and *LS*) to the system which correspond to animal motion in the environment[4]. Firstly, the animal's motion in straight line along the preferred direction of a ring of stripe cells, secondly that along a circle and finally that in open space was coded in Verilog to provide inputs to the 3 stripe cell rings. Neuron numbers from the stripe cell ring chips were read using the FPGA and according to the GRIDSmap model, inputs were sent to 3 grid synapse-neuron circuits to demonstrate 3 different spatial firing frequencies. Outputs from these 3 grid cells were directly provided as inputs to the Bayesian synapse circuit on the place chip. Test results from the individual circuits have been reported in [46], [49], [51]. Thus, this paper specifically presents their use as a part of the hippocampal formation which is the first time as far as our knowledge of literature goes. Parameters used for these tests are shown in Table 1 in Appendix.

6.1 *Motion in straight line*

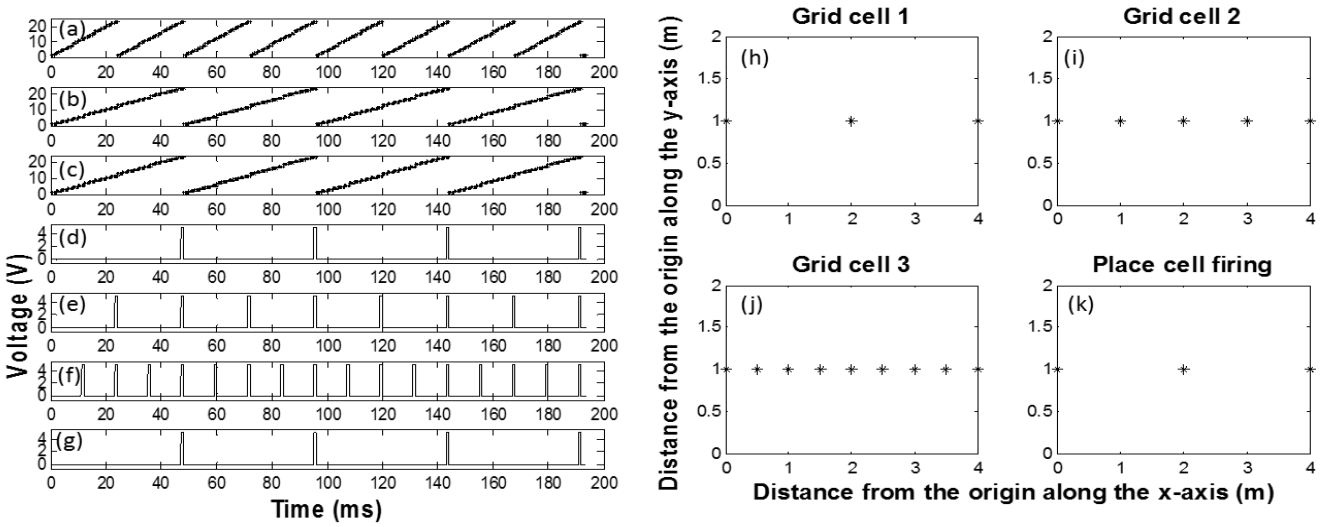

Fig. 12 Measurement results from the system as the animal moves along the preferred firing direction of one of the ring of stripe cells. (a) Ring numbers of the ring along which the direction of motion is aligned. The neurons numbers move from 1→2→….. →24→ 1 and so on at 1kHz, (b) and (c) show movement of winning node position along the other 2 rings which are aligned at 60 and -60 degrees to the first one. The rate of movement along these is half of that along the first one because cos (60) is 0.5. (d)-(f) Show the grid cell firing pattern of different frequencies which is obtained when (d) the neuron numbers 24 on all the three rings fire simultaneously and provide input to the grid cell or when (e) either 12 or 24 neuron numbers on all the rings fire simultaneously and provide input to the grid cell or when (f) either 6, 12, 18 or 24 neuron numbers fire simultaneously and provide inputs to the grid cell. (g) The place cell fires when all the grid cell inputs to it are coincident. (h)-(k) Showing extrapolation of place cell firing (*) in the x-y plane as the animal motion along the preferred firing direction of a ring is simulated.

When an animal moves around in space, according to the GRIDSmap model (section 3.1), location of the animal in space shall be mapped on to neurons in the stripe cell rings. For simplicity, here we consider the case of only the 3 stripe cell rings which are connected to the 3 grid cell neurons that we are using in our system design. Since we are first considering the case where animal motion along a straight line is simulated, the position of the winning node will change on one of the rings (say ring1) at a particular rate and that along the other two at half of that rate because the rings are aligned at 60 degrees to each other and cos (60) is 0.5. We also assume here that the movement along the 24 nodes of a ring wraps around after 1m. To implement this on our silicon system, we applied a right shift (*RS*) signal to one of the rings at 1kHz, and at 500 Hz to the second and the third rings. The corresponding neurons which fired on all the rings were read using the FPGA board. Through this software interface, node 24 of all the rings was attached to a grid cell neuron through a second order synapse circuit. Thus, this grid cell neuron was expected to fire after every 2m of distance travelled by the animal in space. Another grid cell neuron was connected to nodes 12 and 24 of all the three rings. Thus, this should fire after every 1m. Similarly, the grid cell neuron connected to nodes 6, 12, 18 and 24 shall fire every 0.5m of distance covered by the animal along the straight line. Since these three grid cell neurons are connected to a single place cell neuron through a Bayesian integration synapse, the place cell neuron is expected to fire every 2m, i.e., when it receives inputs from all the grid cell neurons at the same time.

[4] Since the hippocampal formation cells fire when the animal moves around and is at particular locations in space, this simulation of animal motion using this silicon system of chips was essential. Even though we tested the network here, the inputs to it were provided as a real neural network would receive when the animal is moving around in the environment.

Thus, the system was provided inputs as *RS* and *LS* signals to the stripe cell ring circuits. The output from the 3 stripe cell ring circuits was read (using the FPGA board) as neuron number which fires at a given time. The neuron numbers recorded from the ring 1 chip and plotted in MATLAB are shown in Fig. 12 (i) (a). The neuron numbers on ring1 are moving from 1→2→….. →23→24→1→ and so on at 1kHz while that on (b) and (c) are moving around at 500 Hz. The FPGA board was programmed to provide inputs to grid cell1 whenever the neuron numbers on all 3 rings were detected to be 24 at the same time, to grid cell2 whenever the neuron number on the rings were either 24 or 12 and grid cell3 when the neuron numbers were either 6, 12, 18 or 24. The subsequent grid cell firing pattern was recorded using the mixed signal oscilloscope (Fig. 12(i) (d-f)) and routed to the place cell neuron circuit through the Bayesian integration synapse circuit. Firing of the place cell neuron was also recorded using the mixed signal oscilloscope (Fig. 12 (i) (g)). The results show firing of grid cell 1 at regular intervals of 2m, of grid cells 2 and 3 at intervals of 1 and 0.5 m respectively, and that of the place cell when all three of them are coincident, as expected by the model. Based on the chip results, projections were made to x-y plane (using MATLAB - Fig. 12 (ii)). The results show that the system can correctly replicate the expected regular spatial firing patterns of the grid cells and place cells when animal motion along a straight line is simulated.

6.2 *Motion in a circle*

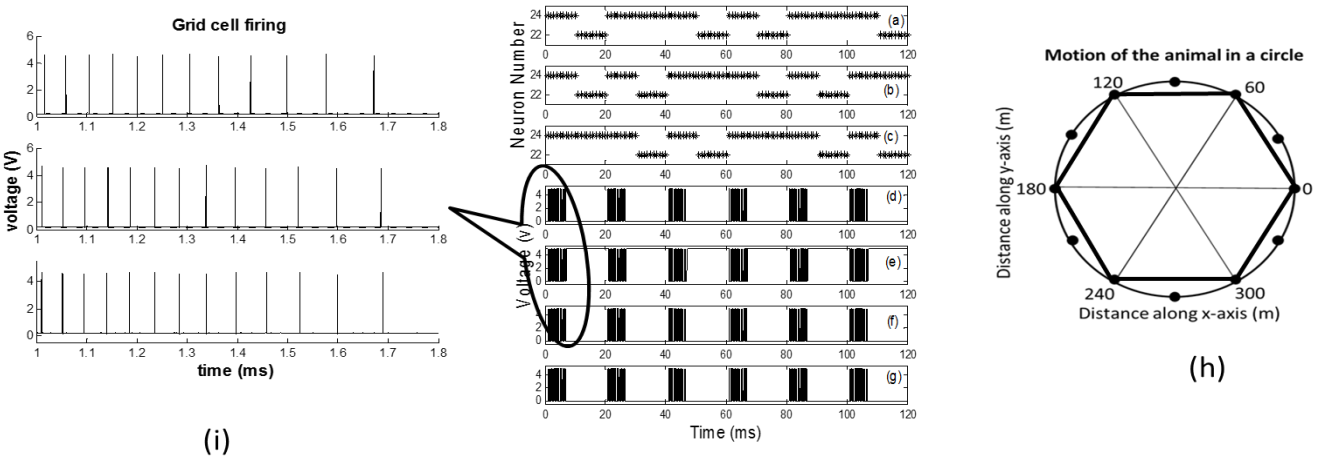

Fig. 13 (a)-(c) Movement of winning node along the 3 stripe cell rings as the animal motion along a circle is simulated (neuron numbers of the 3 rings are shown). Also seen are (d)-(f) the corresponding firing patterns of 3 grid cells (shown in detail in (i)) and that of a (g) place cell. (h) Showing the measured place cell and grid cell firing (*) when animal motion along a circle is simulated. This is a plot in Matlab based on the data obtained from the chips.

Next, we measured the grid and the place cell firing patterns from our silicon hippocampal formation as the animal motion along a circle of radius 2m was simulated. If the animal moves in a circle of radius 2m, then there will be at least 6 points on that circle which shall fall on the edges of a regular hexagon with each edge 2m long (Fig. 13(h)). To extrapolate the animal motion in space on to the 3 rings of stripe cells which are connected to a single grid cell, we took these 6 points. At each of these points, according to the GRIDSmap model, the distance travelled along the direction of the ring on which the point falls shall be 2m while along the other two it shall be 1m. This is because these are aligned at 60 and -60 degrees to the first ring. Thus, the distance covered along these two axis shall be half (cos (60) is 0.5) of 2m or it will be 1m. This corresponds to node position of 24 on all the rings in hardware circuits (assuming the motion wraps around the ring after every 1m). To illustrate motion along the ring, we also picked another 6 points on the ring which were midway between these 6 points. Whenever the animal is at one of these points, say the 90 degree point, the projection of distance to one of the axis shall be 0 (2*cos (90)) and along the other two will be about 1.8 m (2*cos (30)). This shall correspond to node numbers 24 on the former ring and node numbers 22 on the other two. For the other 5 points also the mapping will be similar with alternation in the ring number whose node 24 is active at that point, i.e., [22, 22, 24], [24, 22, 22] or [22, 24, 22] for these 6 positions on the circle which are exactly half way between the former 6 points.

To implement it in our silicon chip system, the position of winning nodes on the three rings was shifted by providing *LS* or *RS* signals to the ring from the FPGA. As described in the section on circuits, these signals were routed through the decoder such that the address of the *LS* or *RS* signals was set and then the *req/* bit of the decoder was pulled active low. As the rings were moved, the neuron numbers were recorded. If the neuron numbers of all the rings were 24, then the synapse of grid cell1 was sent a spike as a result of which it fired. Similarly, spike inputs were sent to grid cell2 if either of the neuron numbers 12 or 24 and to grid cell3 if either of the neuron numbers 6, 12, 18 or 24 from all the rings fired simultaneously. Since, the neuron numbers 6, 12 or 18 on the rings did not fire in this case, all the three grid cells as well as the place cell firing had similar spatial scaling (Fig. 13). Measurement results in Fig. 13 show the

firing pattern when these grid cell outputs were integrated onto the place cell. Hence, this system can correctly track the motion of the animal using the place and the grid cell spatial firing patterns.

6.3 *Motion in open space*

To cover the entire space with animal motion, we simulated motion of the animal (Fig. 14) along one axis for 4 m, then along an axis at 60 degree to this one for 1 m, then in opposite direction for another 4 m and repeated this pattern over and over. So the animal's position at representative points for all places in space was mapped on to the 3 stripe cell rings. According to the GRIDSmap model, during the initial 4 m, node positions along one of the rings (in line with axis of movement) will move around at (say) 1kHz while that along the other 2 will move at half of that rate i.e., at 500 Hz (because cos(60)=0.5). And the nodes were moved around such that the motion wrapped around after every 1m. For the next 1 m when animal motion in the direction of the second ring was simulated, the position of the winning node will move on this ring by 1m and by 0.5 m along the other two rings (as these will be now at 60 degrees to the direction of motion and cos(60) is 0.5). To implement this in our silicon system of chips, firstly ring 1 was moved 96 positions to the right (by providing 96 *RS* signals), rings 2 and 3 by 48 positions to the right. Then node positions on rings 1 and 3 were shifted 12 positions to the right and the left respectively and that on ring 2 by 24 positions to the right. Then the animal motion along the direction of the first ring for 4 m but in opposite direction was simulated. This corresponds to movement in opposite direction for 96 positions along ring 1 (using *LS* signals), by 48 positions to the left for both rings 2 and 3. This pattern of movement along the rings was repeated over and over so as to cover the entire space with animal motion.

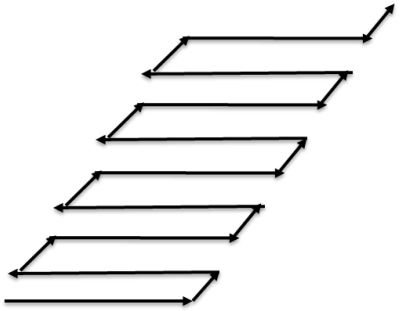

Fig. 14 Schematic showing the animal trajectory simulated on the chip to obtain the results shown in Fig. 15.

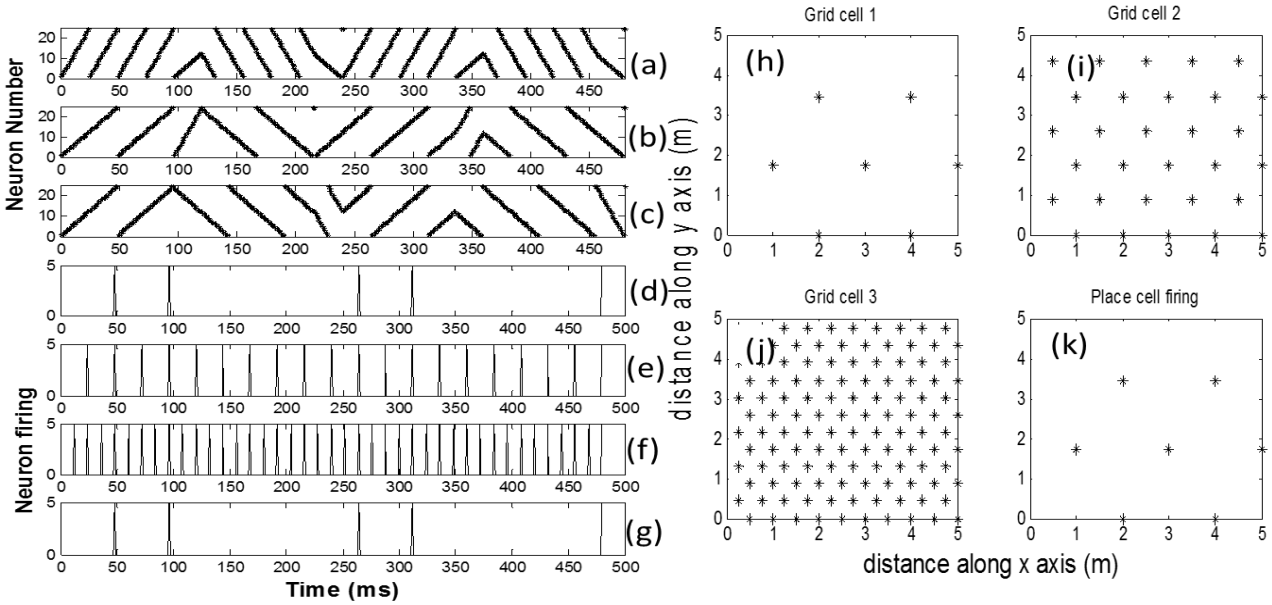

Fig. 15 Measurement results from (a)-(c) 3 stripe cell rings, (d)-(f) 3 grid cells and one (g) place cell when animal motion in open space is simulated. (a)-(c) Neuron numbers of the 3 stripe cell rings as the animal moves around in space. (d)-(f) The results show firing of grid cells at regular intervals with different scaling. (g) The place cell fires when it gets inputs from all the grid cells simultaneously. (h)-k) Grid and place cell firing (*) extrapolated from that recorded from the chips as the animal motion in open space is simulated.

Thereafter, using the software interface in FPGA, the first grid cell was connected to neuron number 24 of each ring, second grid cell to neuron numbers 12 and 24 and the third grid cell to neuron numbers 6, 12, 18 and 24 of each of the rings. The place cell fired only when it received inputs from all the three grid cells. Detailed grid firing pattern of different spatial frequencies and that of place cell was projected to entire space and plotted in MATLAB (Fig. 15 (h)-(k)). One snippet of the recordings from the 3 chips, as seen on the oscilloscope and later processed in MATLAB, is shown in Fig. 15 (a-g). As the environment is scaled to bigger size, the grid cell and the place cell firing shall just extend in a similar pattern, i.e., the hexagonal pattern shall be preserved even though it will spread out to the entire space. These results demonstrate that we could successfully achieve the function of the hippocampal formation based on the models with these 3 chips/circuits in silicon. In all these tests, we demonstrated place cell firing based on grid cell firing as per the GRIDSmap model extended to explain place cell firing based on Bayesian integration. Even though the grid cell spatial frequencies chosen here are multiples of each other, in reality, they may not be so. Therefore, even though here it seems that the place cell firing is a function of grid cell firing of the highest spatial frequency alone, it might not be the case. For instance, if the spatial firing frequencies of the 3 grid cells were 1m, 3m and 8m, then the place cell shall fire after every 24 m which is not equivalent to the spatial firing frequency of either one alone.

7 Conclusion

In this paper, we integrated 3 silicon chips fabricated using 0.5 µm ON semiconductor technology into a system which mimics the spatial navigation function of the hippocampal formation based on the GRIDSmap model and Bayesian integration. With the circuits on the chips, we could realize the function of the stripe cells ring which could perform motion integration. Three stripe cells from these rings were connected to a grid neuron through a second order synapse circuit to demonstrate firing patterns with a spatial frequency of 1m. Multiples of this frequency were obtained by connecting more stripe cells with 2 other grid cells. Thus, we could demonstrate the hexagonal firing patterns of the entorhinal cortex grid cells with different spatial frequencies as per the GRIDSmap model. As far as our knowledge of literature, this is the first such demonstration of grid cell firing in silicon. Further, we extended the idea of Bayesian integration as a possible mechanism for input integration in place cells formed based on the GRIDSmap model. To implement it in silicon, we designed and fabricated a circuit which can perform Bayesian integration and demonstrated results from chip measurements. Hence, in this work, we could demonstrate the working of the hippocampal formation from the perspective of the GRIDSmap model in silicon. This system is capable of learning new paths (by changing connections between stripe cells and grid cells) and encoding for the animal's position in space. As seen above, our system is based on mathematical models of the hippocampal formation. Thus, it correctly implements in silicon what the models describe to be the computational basis of the spatial firing patterns of the cells of the hippocampal formation. Grid cell mathematical models are capable of describing the empirically observed patterns quite successfully but the place cell computational models need more refinement. Results obtained here in silicon can also help refine the current place cell models by providing better insights into them. Future work in this field involves developing a more empirically plausible mathematical model explaining the hippocampal place cell firing. Towards this goal, we have come up with a sensorimotor model of the place cells [52], [53] which is closer to the empirical observations than the current models of place cells. The sensorimotor model can also be implemented using the above hardware system. Another noteworthy fact is that like any other prior implementation of a biological system in silicon [3] or like the actual biological systems, our system also suffered from drift due to noise, mismatch, etc., when we tried to integrate motion for a longer duration, i.e., over an hour. To correct this, we repeatedly reset the rings to node 1 using inputs from the FPGA to the ring circuits. This corrected the error and enabled the system to perform path integration and spatial mapping accurately over extended periods of time and space.

Acknowlegements

This work was performed in the lab of and under the supervision of Prof Robert W. Newcomb at the University of Maryland, College Park, MD. An earlier version of the stripe cell ring circuit was developed by the author in the lab of Prof T. K. Horiuchi.

Appendix

Table1 Parameters used for testing the system

Chip	Parameter	Voltage (V)
Stripe cells' ring chip	*V2*	4.15
	V1	3.9
	V_{leak} *(ring)*	0.40
	V_{bias}	1.46
	cCon	4.17
	V_{lk}*(neuron)*	0.52
	V_{refr}	0.5
Grid cell	V_{syn}	2.6

chip	$V_{τ1}$	3.5
	$V_{τ2}$	4.5
	V_f	2.88
	V_s	3.79
	V_{we}	4.1
	V_{lk}	4.29
	V_{refr}	4.38
	V_{thr}	0.75
Place cell chip	V_{bias}	1.5
	V_{thr}	0.6
	V_{lk}	4.41
	V_{we}	4.05
	V_{refr}	4.26

REFERENCES

[1] D. Purves, G. J. Augustine, D. Fitzpatrick, W. C. Hall, A. S. LaMantia, and L.E. White, 2012, "*Neuroscience*", 5th edition, Sinauer Associates, Sunderland, MA, USA.

[2] M. Hasselmo, 2012, "*How we remember*", MIT press Cambridge MA.

[3] T.M. Massoud, T.K. Horiuchi, 2011, "A neuromorphic VLSI head direction cell system", *IEEE Trans. Circuits and Systems I*, 58(1), 150-163

[4] T.M. Massoud, T.K. Horiuchi, 2012, "A neuromorphic VLSI grid cell system", *International Symposium for Circuits and Systems (ISCAS),* 2012.

[5] N Burgess, J O'Keefe, 2002, "Spatial Models of the Hippocampus," in *The Handbook of Brain Theory and Neural Networks, 2nd Edition* Ed: Arbib M A, MIT press, Cambridge MA.

[6] J. S. Taube, R. U. Muller, J. B Ranck., Jr., 1990, "Head direction cells recorded from the postsubiculum in freely moving rats. I. Description and quantitative analysis", *J Neurosci* 10: 420-435

[7] J. S. Taube, R. U. Muller, J. B Ranck., Jr., 1990, "Head direction cells recorded from the post-subiculum in freely moving rats. II. Effects of environmental manipulations", *J Neurosci.* 10: 436-447.

[8] T. Hafting, M. Fyhn, S. Molden, M. B. Moser., E. I. Moser, August 2005, "Microstructure of a spatial map in the entorhinal cortex", *Nature*, Vol. 436, 801-6.

[9] J. O'Keefe and D.H. Conway, 1978, "Hippocampal Place Units in the freely moving rat: Why they fire where they fire", *Exp. Brain Res*. 31, 573-590.

[10] J. O'Keefe, 1976, "Place units in the hippocampus of the freely moving rat", *Exp. Neurol.* 51, 78-109.

[11] J. O'Keefe, D. Conway, 1976, "Sensory inputs to the hippocampal place units", *Neurosci. Letters* 3. 103-104.

[12] J. O'Keefe, L. Nadel, 1977, " *The Hippocampus as a cognitive map*", Oxford, Clarendon Press.

[13] J. O'Keefe, & J. Dostrovsky, 1971, "The hippocampus as a spatial map Preliminary evidence from unit activity in the freely moving rat", *Brain Res*, 34 (1), 171-175.

[14] J. O'Keefe, 1976, "Place units in the hippocampus of the freely moving rat", *Exp. Neurol.* 51, 78-109.

[15] M. C. Fuhs, D. S. Touretsky, 2006, "A spin glass model of path integration in rat medial entorhinal cortex", *Jour. Neuroci*., 26(16), 4266-4276.

[16] Y. Burak, I. Fiete, 2006, "Do we understand the emergent dynamics of grid cell activity?" *Jour. Neurosci.,* 26(37), 9352-9354.

[17] Y. Burak, I. R. Fiete, 2009, "Accurate path integration in continuous attractor network models of grid cells", *Comp. Bio*., 5(2), 1-16, e1000291.

[18] N. Burgess, C. Barry, J. O'Keefe, 2007, " An oscillatory interference model of grid cell firing", *Hippocampus,* 17, 801-812.

[19] J. O'Keefe, N. Burgess, 2005, "Dual phase and rate coding in hippocampal place cells: theoretical significance and relationship to entorhinal grid cells", *Hippocampus,* 15, 853-866.

[20] D. Bush, N. Burgess, 2014, "A hybrid oscillatory interference /continuous attractor network model of grid cell firing", *Jour. Neurosci.,* 34(14), 5065-5079.

[21] H. Mhatre, A. Gorchetchnikov, and S. Grossberg, 2012, "Grid Cell Hexagonal Patterns Formed by Fast Self-Organized Learning within Entorhinal Cortex", *Hippocampus*,, 22, 320–334.

[22] C. Barry, C. Lever, R. Hayman, T. Hartley, S. Burton, J. O'Keefe, K. Jeffery and N. Burgess, 2006, "The boundary vector cell model of place cell firing and spatial memory", *Rev. Neurosci*., 17 (1-2), 71-97.

[23] T. Hartley, N. Burgess, C. Lever, F. Cacucci, J. O'Keefe, 2000, "Modeling place fields in terms of the cortical inputs to the hippocampus", *Hippocampus*, 10, 369-379.

[24] T. Solstad, E. I. Moser, G. T. Einevoll, 2006, "From grid to place cells: A mathematical model", *Hippocampus*, 16, 1026-1031.

[25] S. Cheng, L. M. Frank, 2011, "The Structure of networks that produce the transformation from grid cells to place cells", *Neuroscience*, 197, 293-306.

[26] E. T. Rolls, S. M. Stringer, T. Elliot, 2006, "Entorhinal cortex grid cells can map to hippocampal place cells by competitive learning", *Network*, 17, 447-465.

[27] A. Gorchetchnikov, S. Grossberg, 2007, "Space, time and learning in the hippocampus: how fine spatial and temporal scales are expanded into population codes for behavioral control", *Neural Netw*., 20, 182-193.

[28] C. Molter, Y. Yamaguchi, 2008, "Entorhinal theta phase precession sculpts dentate gyrus place fields", *Hippocampus*, 18, 919-930.

[29] B. Si, A. Treves, 2009, "The role of competitive learning in the generation of DG fields from EC inputs", *J. Neurophysiol.* , 103, 3167-3183.

[30] L. de Almeida, M. Idiart, J. E. Lisman, 2009, "The input-output transformation of the hippocampal granule cells: from grid to place fields", *J. Neurosci*, 29, 7504-7512.

[31] J. D. Monaco, L. F. Abbott, 2011, "Modular realignment of entorhinal grid cell activity as a basis for hippocampal remapping", *J. Neurosci*., 31, 9414-9425.

[32] M. Franzius, R. Vollgraf, L. Wiscott, 2007, "From grids to places", *J. Comput. Neurosci.*, 22, 297-299.

[33] F. Savelli, J. J. Kneirim, 2010, "Hebbian analysis of the transformation of medial entorhinal grid cell inputs to hippocampal place fields", *J. Neurophysiol.* 103, 3167-3183.

[34] B. Poucet, F. Sargolini, E. Y. Song, B. Hangya, S. Fox and R. U. Muller, 2014, "Independence of landmark and self-motion guided navigation: a different role for grid cells", *Phil. Trans. R. Soc. B,* 369, 20130370.

[35] D. Bush, C. Barry, N. Burgess, 2014, "What do grid cells contribute to place cell firing?", *Cell,* 37(3), 136-145.

[36] D. C. Knill, A. Pouget, 2004, "The Bayesian Brain: the role of uncertainty in neural coding and computation", *Trends in Neurosci.,* 27(12) 712-719.

[37] M. Colombo, P. Series, 2012, "Bayes in the brain-on Bayesian modelling in Neuroscience", *Brit. J. Phil. Sci.,* 63, 697-723.

[38] M. O. Ernst, M. S. Banks, 2002, "Humans integrate visual and haptic information in a statistically optimal fashion", *Nature*, 415 (24), 429-433.

[39] K. P. Kording, D. M. Wolpert, 2004, "Bayesian integration in sensorimotor learning", *Nature,* 427, 244-7.

[40] W. J. Ma, J. M. Beck, A. Pouget, 2008, "Spiking networks for Bayesian inference and choice", *Curr. Opi. In Neurobio.,* 18, 217-222.

[41] R. S. Zemel, P. Dayan, A. Pouget, 1998, "Probabilistic interpretation of population codes", *Neural Computation,* 10, 403-430.

[42] G. Pfuhl, H. Tjelmeland, R. Biegler, 2011, "Precision and reliability in animal navigation", *Bull Math Biol.,* 73, 951-977.

[43] P. R. MacNeilage, N. Ganesan, D. E. Angelaki, 2008, "Computational approaches to spatial orientation: from transfer functions to dynamic Bayesian inference", *J. Neurophysiol*, 100, 2981-2996.

[44] T. Madl, S. Franklin, K. Chen, D. Montaldi, R. Trappl, 2014, "Bayesian integration of information in hippocampal place cells", *PLOS one,* 9(3), e89762.

[45] MATLAB R2011b. Available at <http://www.mathworks.com> Accessed 01/03/14.

[46] A.Aggarwal, 2015, "Neuromorphic VLSI Bayesian integration synapse", the *Electronics letters*, 51(3), 207-209.

[47] J. Lazzaro, S. Ryckebusch, M. A. Mahowald, C. A. Mead, 1989, " Winner take all networks of O(n) complexity", *Advances in Neural Information Processing Systems*, 1, 703-711, San Mateo, CA. Morgan Kaufmann.

[48] K. A. Boahen, 1998, "Communicating Neuronal Ensembles between Neuromorphic Chips", *Neuromorphic Systems Engineering*, The Springer International Series in Engineering and Computer Science, 447, 229-259.

[49] A. Aggarwal, T.K. Horiuchi, 2015, "A neuromorphic VLSI second order synapse", the *Electronics Letters*, 51(4), 319-321.

[50] S. C. Liu, J. Kramer, G. Indiveri, T. Delbruck, R. Douglas, 2002, "*Analog VLSI: Circuits and principles*", the MIT press, Cambridge, MA pp 168-175.

[51] A.Aggarwal, 2015, "VLSI realization of neural velocity integrator and central pattern generator", the *Electronics Letters*, available at < http://digital-library.theiet.org/content/journals/10.1049/el.2015.0544>.

[52] A. Aggarwal, 2015, "The sensorimotor model of the hippocampal place cells", Abstract, *24th Annual Computational Neurosci. Meeting, CNS Prague, July 18-23, 2015, Prague, Czech Republic, BMC Neuroscience,* 16(Suppl 1):P2

[53] A. Aggarwal, 2016, "The sensori-motor model of the hippocampal place cells", *Neurocomputing*. <http://dx.doi. org/10.1016/j.neucom.2015.12.044i Neurocomputing>